

Magnetic control of nonlinear transport induced by the quantum metric

Xu Chen,¹ Mingbo Dou,¹ Qin Zhang,¹ Xianjie Wang,^{1,2,3} M. Ye. Zhuravlev,⁴ A. V. Nikolaev,⁵ and L. L. Tao^{1,2,3,*}

¹School of Physics, Harbin Institute of Technology, Harbin 150001, China

²Frontiers Science Center for Matter Behave in Space Environment,
Harbin Institute of Technology, Harbin 150001, China

³Heilongjiang Provincial Key Laboratory of Advanced Quantum Functional Materials and Sensor Devices, Harbin 150001, China

⁴Faculty of Liberal Arts and Sciences, St. Petersburg State University, St. Petersburg 190000, Russia

⁵Skobeltsyn Institute of Nuclear Physics, Moscow State University, Moscow 101000, Russia

(Dated: July 15, 2025)

The quantum geometry plays a crucial role in the nonlinear transport of quantum materials. Here, we use the Boltzmann transport formalism to study the magnetic control of nonlinear transport induced by the quantum metric in two-dimensional systems with different types of spin-orbit coupling (SOC). It is shown that the nonlinear conductivity is strongly dependent on the direction of a field and reveals significant spatial anisotropy. Moreover, the field-direction dependent relations are distinct for different SOCs. In addition, it is demonstrated that the contributions from the quantum metric and Drude mechanism are distinguishable due to their opposite signs or distinct anisotropy relations. We further derive the analytical formulas for the anisotropic nonlinear conductivity, in exact agreement with numerical results. Our work shines more light on the interplay between the nonlinear transport and quantum geometry.

I. INTRODUCTION

The nonlinear transport due to the *intrinsic* quantum geometry of wave functions has attracted growing interest[1–6]. For example, it was predicted[7, 8] that the Berry curvature dipole (BCD) in \mathcal{T} -invariant (\mathcal{T} for time reversal) materials can induce a nonlinear anomalous Hall effect (NLAHE), which was experimentally observed in Weyl semimetals WTe₂ and MoTe₂[9–11]. In addition, the *intrinsic* NLAHE can be induced by the quantum metric[12], as demonstrated in antiferromagnets CuMnAs[13], Mn₂Au[14], MnBi₂Te₄[15], manganese chalcogenides MnX (X=S, Se, Te) monolayer[16], and the altermagnet RuO₂[17]. Inversely, measuring the NLAHE is useful to probe the quantum geometry in quantum materials and can also be exploited to detect the direction of Néel vector in antiferromagnets[13, 14, 16]. Recently, the displacement current under an AC electric field driven by the quantum metric was demonstrated and its quantum theory was formulated[18].

It is known that the second-order nonlinear conductivity $\sigma_{abc}^{(2)}$ ($a, b, c = x, y, z$ for Cartesian components) characterizing the nonlinear transport has three contributions[19–21]: the nonlinear Drude conductivity $\sigma_{abc}^{\text{Drude}}$ caused by the band asymmetry, the BCD induced nonlinear conductivity $\sigma_{abc}^{\text{BCD}}$ and the quantum metric induced nonlinear conductivity σ_{abc}^{QM} . Importantly, $\sigma_{abc}^{\text{BCD}}$ represents a purely transverse effect while $\sigma_{abc}^{\text{Drude}}$ and σ_{abc}^{QM} have both transverse and longitudinal effects due to their identical symmetry restrictions[19–21]. In earlier studies[12–14], it was indicated that σ_{abc}^{QM} contributes only to the transverse response while the longitudinal component is vanishing. Recent works[19, 20] show that σ_{abc}^{QM} also contributes the longitudinal nonlinear transport and the quantum metric dominated nonreciprocal charge transport was observed in MnBi₂Te₄ thin films[22]. On the other hand, $\sigma_{abc}^{\text{Drude}}$,

$\sigma_{abc}^{\text{BCD}}$ and σ_{abc}^{QM} have distinct relaxation time τ dependent relations: $\sigma_{abc}^{\text{Drude}}$ and $\sigma_{abc}^{\text{BCD}}$ are τ^2 and τ dependent, respectively, while σ_{abc}^{QM} is τ independent. Thus, σ_{abc}^{QM} dominates the nonlinear transport in the dirty limit ($\tau \rightarrow 0$) and represents an *intrinsic* contribution to the nonlinear transport.

The nonreciprocal charge transport (NCT)[23–25] is characterized by different resistances for opposite currents and can be described by the longitudinal nonlinear conductivity $\sigma_{aaa}^{(2)} = \sigma_{aaa}^{\text{Drude}} + \sigma_{aaa}^{\text{QM}}$ due to the vanishing of $\sigma_{aaa}^{\text{BCD}}$. Both \mathcal{P} (\mathcal{P} for inversion) and \mathcal{T} symmetries must be broken to obtain nonzero $\sigma_{abc}^{\text{Drude}}$ or σ_{abc}^{QM} . Indeed, the sizable NCT effect due to $\sigma_{abc}^{\text{Drude}}$ was observed in ferromagnetic/antiferromagnetic materials[26–28] and non-magnetic materials without \mathcal{P} symmetry by applying an external magnetic field[29–35]. In those systems, the band asymmetry responsible for $\sigma_{abc}^{\text{Drude}}$ is caused by the combined spin-orbit coupling (SOC) and magnetic field. Recently, we studied the anisotropic nonlinear Drude conductivity based on the Boltzmann transport theory[36]. It was shown that the nonlinear Drude conductivity reveals significant spatial anisotropy and different SOCs reveal distinct field-direction dependent relations. In this work, we focus on the anisotropic nonlinear conductivity induced by the quantum metric.

The rest of the paper is organized as follows. In Sec. II, we present the theoretical formalism and general formula for the nonlinear conductivity calculations. In Sec. III, we discuss the magnetically tunable anisotropic nonlinear conductivity based on the general Hamiltonian model. Finally, Sec. IV is reserved for further discussion and conclusion.

II. THEORETICAL FORMALISM

The starting point is the following Hamiltonian describing the two-dimensional (2D) system with SOC and Zeeman

* Contact author: lltao@hit.edu.cn

TABLE I. The derived $\sigma_{\phi\phi\phi}^{\text{Drude}}$ and $\sigma_{\phi\phi\phi}^{\text{QM}}$ for different SOCs within the weak-field or high-density regime. $\Omega(\mathbf{k})$ is the corresponding spin-orbit field and $\alpha, \beta, \gamma, \delta$ are the SOC parameters. The prefactors $\sigma_{R/D/W/P}^{\text{Drude}}$ are given in Ref. [36] while $\sigma_{R/D/W/P}^{\text{QM}}$ are given in the main text.

SOC	$\Omega(\mathbf{k})$	$\sigma_{\phi\phi\phi}^{\text{Drude}} \text{[36]}$	$\sigma_{\phi\phi\phi}^{\text{QM}}$
RSO	$\alpha(-k_y, k_x, 0)$	$\sigma_R^{\text{Drude}} \sin \theta \sin(\varphi - \phi)$	$\sigma_R^{\text{QM}} \sin \theta \sin(\varphi - \phi)$
DSO	$\beta(k_x, -k_y, 0)$	$\sigma_D^{\text{Drude}} \sin \theta \cos(\varphi + \phi)$	$\sigma_D^{\text{QM}} \sin \theta \cos(\varphi + \phi)$
WSO	$\gamma(k_x, k_y, 0)$	$\sigma_W^{\text{Drude}} \sin \theta \cos(\varphi - \phi)$	$\sigma_W^{\text{QM}} \sin \theta \cos(\varphi - \phi)$
PSO	$\delta(k_x - k_y, k_x - k_y, 0)$	$\sigma_P^{\text{Drude}} \sin \theta \sin(\varphi + \frac{\pi}{4}) \sin(\phi - \frac{\pi}{4})$	$\sigma_P^{\text{QM}} \sin \theta \sin(\varphi + \frac{\pi}{4}) \sin^3(\phi - \frac{\pi}{4})$

effects[36, 37]:

$$\mathcal{H} = \frac{\hbar^2 k^2}{2m_e} + \Omega(\mathbf{k}) \cdot \sigma - \Delta \hat{\mathbf{m}} \cdot \sigma, \quad (1)$$

The first term represents the kinetic energy given in terms of electron effective mass (isotropic approximation) m_e , the reduced Planck's constant \hbar , and the wave vector $\mathbf{k} = (k_x, k_y) = k(\cos\phi, \sin\phi)$ in the Cartesian and polar coordinates (ϕ for azimuthal angle). The second term describes the SOC with $\Omega(\mathbf{k}) = (\Omega_x, \Omega_y, \Omega_z)$ and $\sigma = (\sigma_x, \sigma_y, \sigma_z)$ being the spin-orbit field and the vector of Pauli matrices, respectively. The third term is the Zeeman term, where Δ characterizes the magnitude of the exchange field or an external magnetic field and the unit vector $\hat{\mathbf{m}} = (\sin\theta\cos\varphi, \sin\theta\sin\varphi, \cos\theta)$ (θ for polar angle and φ for azimuthal angle) denotes the direction of a field. It is noteworthy that the exchange field can be induced by a ferromagnetic or antiferromagnetic insulator substrate through the magnetic proximity effect[38]. Equation (1) can be rewritten as $\mathcal{H} = \hbar^2 k^2 / (2m_e) + \mathbf{h}(\mathbf{k}) \cdot \sigma$ with $\mathbf{h}(\mathbf{k}) \equiv \Omega(\mathbf{k}) - \Delta \hat{\mathbf{m}}$ being the effective field. The eigenvalues $\epsilon_{\mathbf{k}s}$ ($s = \pm 1$ for spin index) and normalized eigenstates $\psi_{\mathbf{k}s}$ can be obtained as[39]

$$\begin{aligned} \epsilon_{\mathbf{k}s} &= \frac{\hbar^2 k^2}{2m_e} + sh, \\ \psi_{\mathbf{k}s} &= \frac{e^{i\mathbf{k}\cdot\mathbf{r}}}{\sqrt{2h(h-sh_z)}} \begin{pmatrix} h_x - ih_y \\ sh - h_z \end{pmatrix}. \end{aligned} \quad (2)$$

In this work, we consider four different SOCs, that is, Rashba (RSO)[40–42], Dresselhaus (DSO)[43–45], Weyl (WSO)[46–48], and the SOC with persistent spin texture (PSO)[49–55] as similar to previous works[39, 56, 57] and the corresponding $\Omega(\mathbf{k})$ is listed in Table I.

To second order in an applied electric field \mathcal{E} , the produced current density \mathbf{J} is given by[58]

$$J_a = \sigma_{ab}^{(1)} \mathcal{E}_b + \sigma_{abc}^{(2)} \mathcal{E}_b \mathcal{E}_c, \quad (3)$$

where $\sigma^{(1)}$ and $\sigma^{(2)}$ are the first-order linear and second-order nonlinear conductivities, respectively. The indices $a, b, c = x, y$ denote Cartesian components and a summation over repeated indices is implied. It has been proved that $\sigma_{abc}^{(2)}$ can be

separated into three parts[19, 20]

$$\sigma_{abc}^{(2)} = \sigma_{abc}^{\text{Drude}} + \sigma_{abc}^{\text{BCD}} + \sigma_{abc}^{\text{QM}}. \quad (4)$$

The first term $\sigma_{abc}^{\text{Drude}}$ refers to the nonlinear Drude conductivity. Under the relaxation time τ approximation, $\sigma_{abc}^{\text{Drude}}$ takes the form[59–61]

$$\sigma_{abc}^{\text{Drude}} = -\frac{e^3 \tau^2}{4\pi^2 \hbar^3} \sum_n \int f_n \frac{\partial^3 \epsilon_{n\mathbf{k}}}{\partial k_a \partial k_b \partial k_c} d^2 k, \quad (5)$$

where $f_n(\epsilon_{n\mathbf{k}}, \epsilon_F)$ is the Fermi distribution function given in terms of the eigenvalue of the n th band $\epsilon_{n\mathbf{k}}$ and the Fermi energy ϵ_F . The second term $\sigma_{abc}^{\text{BCD}}$ represents the nonlinear conductivity induced by the Berry curvature dipole (BCD) and reads[7]

$$\sigma_{abc}^{\text{BCD}} = -\frac{e^3 \tau}{4\pi^2 \hbar^2} \sum_n \int f_n \left(\frac{\partial \Omega_n^{ca}}{\partial k_b} + \frac{\partial \Omega_n^{ba}}{\partial k_c} \right) d^2 k, \quad (6)$$

where Ω_n^{ab} is the Berry curvature given by $\Omega_n^{ab} = \partial_{k_a} A_{nn}^b - \partial_{k_b} A_{nn}^a$, with A_{nn}^a being the Berry connection $A_{nn}^a = i\langle n | \partial_{k_a} | n \rangle$ ($|n\rangle$ for the n th Bloch state). It is clearly that $\sigma_{aaa}^{\text{BCD}} = 0$ due to $\Omega_n^{aa} = 0$. Thus, $\sigma_{abc}^{\text{BCD}}$ represents the nonlinear transverse (Hall) effect and does not contribute to the longitudinal nonlinear conductivity. The last term σ_{abc}^{QM} represents the nonlinear conductivity induced by the quantum metric and is given by[20]

$$\sigma_{abc}^{\text{QM}} = -\frac{e^3}{4\pi^2 \hbar} \sum_n \int f_n \left[2 \frac{\partial G_n^{bc}}{\partial k_a} - \frac{1}{2} \left(\frac{\partial G_n^{ca}}{\partial k_b} + \frac{\partial G_n^{ba}}{\partial k_c} \right) \right] d^2 k, \quad (7)$$

where G_n^{ab} is the band-normalized quantum metric or the Berry connection polarizability and reads[14, 20]

$$G_n^{ab} = 2\text{Re} \sum_{m \neq n} \frac{A_{nm}^a A_{mn}^b}{\epsilon_{n\mathbf{k}} - \epsilon_{m\mathbf{k}}}. \quad (8)$$

For the Hamiltonian Eq. (1), the band index n is replaced by the spin index s in Eqs. (5)-(8) and G_s^{ab} can be obtained as[12]

$$G_s^{ab} = s \frac{\partial_{k_a} \hat{\mathbf{h}} \cdot \partial_{k_b} \hat{\mathbf{h}}}{4\hbar}, \quad (9)$$

with the unit vector $\hat{\mathbf{h}} = \mathbf{h}/\hbar$. It is instructive to examine the spatial anisotropy of the nonlinear conductivity. For \mathcal{E} along the ϕ direction, with the aid of directional derivatives and the symmetry of quantum metric, one finds the anisotropic longitudinal nonlinear conductivity $\sigma_{\phi\phi\phi}^{\text{QM}}$

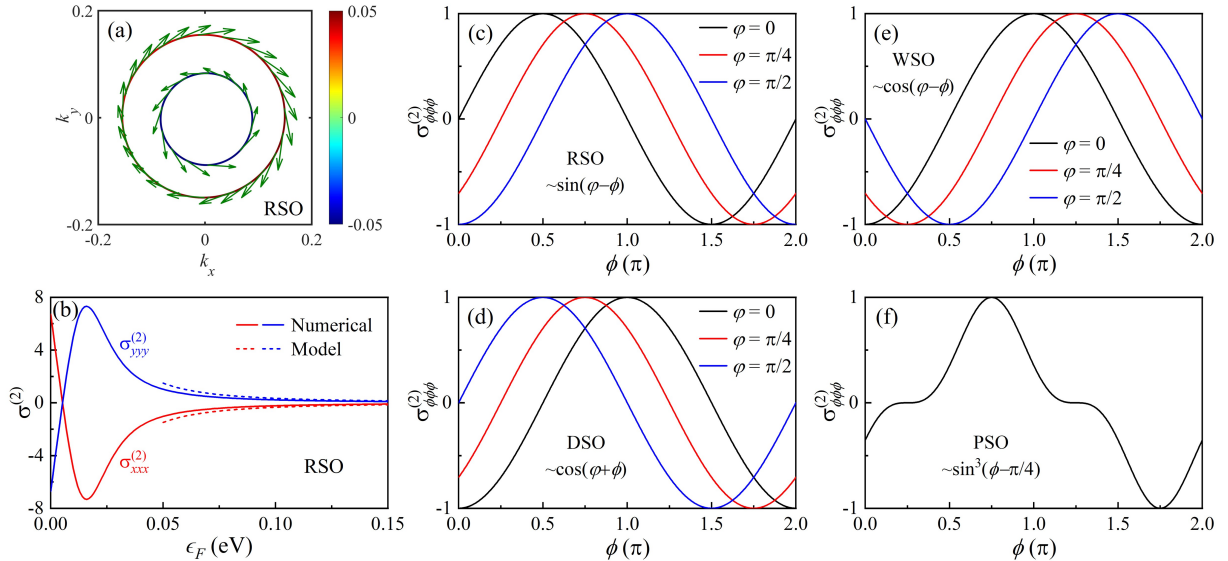


FIG. 1. (a) Fermi contours ($\epsilon_F = 0.1$ eV) for RSO. The in-plane spin textures are indicated by the green arrows while the color map represents the out-of-plane spin polarization. k_x and k_y are in units of \AA^{-1} . (b) The nonlinear conductivity $\sigma_{xxx}^{(2)}$ and $\sigma_{yyy}^{(2)}$ [unit: $10^{-3} e^3 \hbar^3 / (m_e^2 |\alpha|^3)$] for RSO as a function of the Fermi energy ϵ_F . The solid and dashed lines represent the numerical and model results, respectively. Normalized $\sigma_{\phi\phi\phi}^{(2)}$ for RSO (c), DSO (d), WSO (e), and PSO (f) at $\epsilon_F = 0.1$ eV as a function of ϕ for different φ 's. In (a) and (b), θ and φ are fixed as $\theta = \varphi = \pi/4$. In (c)-(f), θ is fixed as $\theta = \pi/4$. The other parameters are assumed to be $m_e = 0.5 m_0$ (m_0 for electron rest mass), $\alpha = \beta = \gamma = \delta = 0.5$ eV \AA , $\Delta = 0.01$ eV, and $T = 50$ K in the Fermi distribution function.

$$\sigma_{\phi\phi\phi}^{\text{QM}} = \sigma_{xxx}^{\text{QM}} \cos^3 \phi + \sigma_{yyy}^{\text{QM}} \sin^3 \phi + (\sigma_{xyy}^{\text{QM}} + 2\sigma_{xxy}^{\text{QM}}) \sin^2 \phi \cos \phi + (\sigma_{yxz}^{\text{QM}} + 2\sigma_{zyx}^{\text{QM}}) \sin \phi \cos^2 \phi. \quad (10)$$

For a given $\Omega(\mathbf{k})$ and so $\mathbf{h}(\mathbf{k})$, one first calculates G_s^{ab} from Eq. (9). Then, σ_{abc}^{QM} can be obtained by plugging G_s^{ab} into Eq. (7). Finally, one obtains $\sigma_{\phi\phi\phi}^{\text{QM}}$ from Eq. (10).

III. ANISOTROPIC NONLINEAR CONDUCTIVITY

In this section, we investigate the anisotropic nonlinear transport by examining the magnetically tunable $\sigma_{\phi\phi\phi}^{(2)}$ based on the Hamiltonian model Eq. (1).

As an illustration, we first examine the nonlinear transport for RSO. Figure 1(a) shows the Fermi contours for RSO at $\epsilon_F = 0.1$ eV and $\theta = \varphi = \pi/4$ and the distorted chiral spin textures can be clearly seen, indicative of band asymmetry along k_x and k_y directions. Figure 1(b) shows the numerically calculated $\sigma_{xxx}^{(2)}$ and $\sigma_{yyy}^{(2)}$ at $\theta = \varphi = \pi/4$ as a function of ϵ_F . One observes that $\sigma_{xxx}^{(2)}$ and $\sigma_{yyy}^{(2)}$ are opposite and reveal slight oscillating behavior for small ϵ_F . As such, $\sigma_{xxx}^{(2)}$ or $\sigma_{yyy}^{(2)}$ reaches its maximum magnitude at $\epsilon_F = 16$ meV. For large ϵ_F , the magnitude of $\sigma_{xxx}^{(2)}$ or $\sigma_{yyy}^{(2)}$ decreases monotonically with increasing ϵ_F , which are in good accordance with model results [see the following Eqs. (12) and (13)].

We then examine the anisotropic nonlinear conductivity $\sigma_{\phi\phi\phi}^{(2)}$ as shown in Fig. 1(c)-(f) for different SOCs. The overall trend is that $\sigma_{\phi\phi\phi}^{(2)}$ is significant anisotropic characterized

by the maximum or zero nonlinear conductivity for certain ϕ 's. Intriguingly, $\sigma_{\phi\phi\phi}^{(2)}$ for RSO, DSO or WSO is θ independent while $\sigma_{\phi\phi\phi}^{(2)}$ for PSO is both θ and φ independent. A detailed examination reveals that $\sigma_{\phi\phi\phi}^{(2)}$ for RSO is proportional to $\sin(\varphi - \phi)$. For other SOCs, we have $\sigma_{\phi\phi\phi}^{(2)} \sim \cos(\varphi + \phi)$ for DSO, $\sigma_{\phi\phi\phi}^{(2)} \sim \cos(\varphi - \phi)$ for WSO and $\sigma_{\phi\phi\phi}^{(2)} \sim \sin^3(\phi - \pi/4)$ for PSO. Such distinct relations offer an efficient way to quantify the SOC type and shall be derived in the following.

We now turn to the magnetically tunable nonlinear conductivity. Without loss of generality, we consider the $\sigma_{yyy}^{(2)}$ component. Figure 2(a)-(d) show the calculated normalized $\sigma_{yyy}^{(2)}$ at $\epsilon_F = 0.1$ eV as a function of (θ, φ) for different SOCs. The overall trend is that $\sigma_{yyy}^{(2)}$ can be significantly tuned by the direction of a field, which is quite similar to that of the nonlinear Drude conductivity[36]. As can be seen, the magnitude of $\sigma_{yyy}^{(2)}$ reaches maximum or zero for certain (θ, φ) 's. In addition, the (θ, φ) dependent relations for different SOCs are distinct. It is seen that $\sigma_{yyy}^{(2)} \sim \sin \theta \sin(\varphi - \pi/2)$ for RSO, $\sigma_{yyy}^{(2)} \sim \sin \theta \cos(\varphi + \pi/2)$ for DSO, $\sigma_{yyy}^{(2)} \sim \sin \theta \cos(\varphi - \pi/2)$ for WSO, and $\sigma_{yyy}^{(2)} \sim \sin \theta \sin(\varphi + \pi/4)$ for PSO. Thus, one can infer the complete (θ, φ) dependent $\sigma_{\phi\phi\phi}^{(2)}$ from Fig. 1(c)-(f) and Fig. 2(a)-(d), that is, $\sigma_R^{(2)} \sim \sin \theta \sin(\varphi - \phi)$, $\sigma_D^{(2)} \sim \sin \theta \cos(\varphi + \phi)$, $\sigma_W^{(2)} \sim \sin \theta \cos(\varphi - \phi)$ and

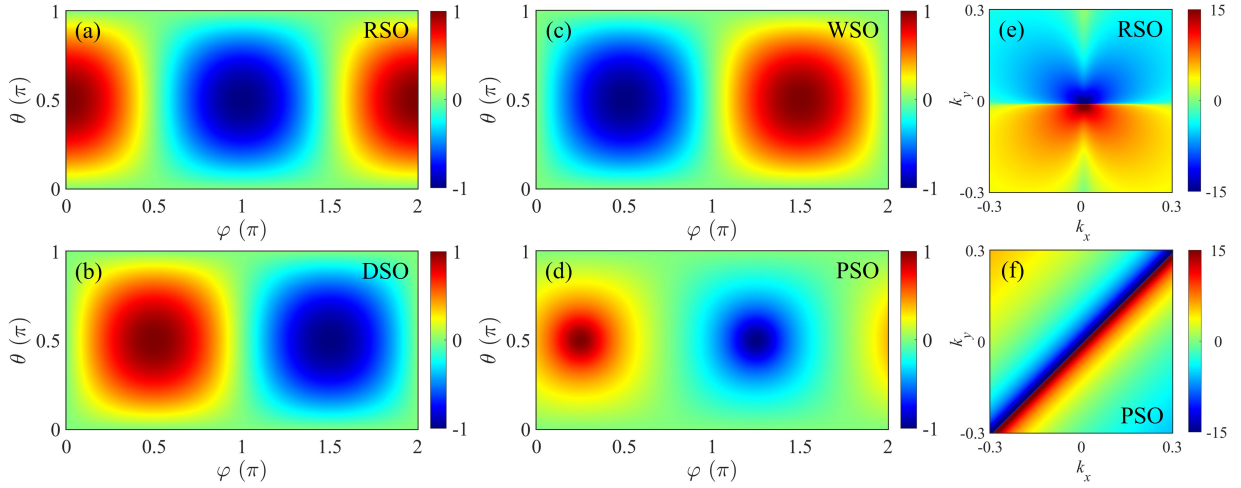


FIG. 2. Normalized $\sigma_{yyy}^{(2)}$ at $\epsilon_F = 0.1$ eV as a function of (θ, φ) for RSO (a), DSO (b), WSO (c), and PSO (d). The \mathbf{k} -resolved $\partial G_+^{yy}/\partial k_y$ at $\theta = \varphi = \pi/4$ for RSO (e) and PSO (f). In (e) and (f), the color map stands for $\ln |\partial G_+^{yy}/\partial k_y| \operatorname{sgn}(\partial G_+^{yy}/\partial k_y)$ and k_x, k_y are in units of \AA^{-1} . The other parameters are assumed to be $m_e = 0.5 m_0$, $\alpha = \beta = \gamma = \delta = 0.5$ eV \AA , $\Delta = 0.01$ eV, and $T = 50$ K in the Fermi distribution function.

$\sigma_P^{(2)} \sim \sin \theta \sin(\varphi + \pi/4) \sin^3(\phi - \pi/4)$. As a comparison, the nonlinear Drude conductivity reveals the same (θ, φ) dependent relations due to their identical symmetry restrictions[36].

On the other hand, from Eq. (7), we have $\sigma_{yyy}^{(2)} \sim \sum_s \int (f_s \partial G_s^{yy}/\partial k_y) d^2k$, it is therefore helpful to examine the \mathbf{k} -resolved $\partial G_s^{yy}/\partial k_y$. For illustration, we consider the higher branch $\partial G_+^{yy}/\partial k_y$ at $\theta = \varphi = \pi/4$ for RSO and PSO. As shown in Fig. 2(e), $\partial G_+^{yy}/\partial k_y$ (logarithmic scale) for RSO

is mainly contributed by the regions around the $\mathbf{k} = \mathbf{0}$ and diagonal lines $k_x = \pm k_y$. In the case of PSO shown in Fig. 2(f), the dominant contributions to $\partial G_+^{yy}/\partial k_y$ are from the regions close to $k_x = k_y$.

Having demonstrated the magnetic control of nonlinear transport based on numerical calculations. We now derive the analytical formulas for $\sigma_{\phi\phi\phi}^{\text{QM}}$ to explain the above observed distinct relations for different SOCs. In a zero-temperature limit, that is, $f_s(\epsilon_{\mathbf{k}s}, \epsilon_F) = \theta(\epsilon_F - \epsilon_{\mathbf{k}s})$, substitution of Eq. (9) in Eq. (7) yields

$$\sigma_{abc}^{\text{QM}} = -\frac{e^3}{4\pi^2\hbar} \int_0^{2\pi} d\phi \int_{k_{F-}}^{k_{F+}} [2 \frac{\partial G_+^{bc}}{\partial k_a} - \frac{1}{2} (\frac{\partial G_+^{ca}}{\partial k_b} + \frac{\partial G_+^{ba}}{\partial k_c})] k dk, \quad (11)$$

where $k_{F\pm}$ are spin-split Fermi wave numbers. In the following derivations, we consider the weak-field or high-density regime, namely $|\alpha|k_F \gg |\Delta|$. For RSO, we obtain

$$\sigma_{\phi\phi\phi}^{\text{QM}} \approx \sigma_R^{\text{QM}} \sin \theta \sin(\varphi - \phi), \quad (12)$$

where the prefactor σ_R^{QM} is defined as

$$\sigma_R^{\text{QM}} = -\frac{5e^3(3\hbar^2\epsilon_F + 2m_e\alpha^2)\Delta}{128\pi\hbar m_e\alpha\epsilon_F^3}. \quad (13)$$

For DSO, we obtain

$$\sigma_{\phi\phi\phi}^{\text{QM}} \approx \sigma_D^{\text{QM}} \sin \theta \cos(\varphi + \phi). \quad (14)$$

For WSO, we find

$$\sigma_{\phi\phi\phi}^{\text{QM}} \approx \sigma_W^{\text{QM}} \sin \theta \cos(\varphi - \phi). \quad (15)$$

In Eqs. (14) and (15), the prefactors σ_D^{QM} and σ_W^{QM} can be obtained by replacing α by β and γ in Eq. (13), respectively. For PSO, we find

$$\sigma_{\phi\phi\phi}^{\text{QM}} \approx \sigma_P^{\text{QM}} \sin \theta \sin(\varphi + \frac{\pi}{4}) \sin^3(\phi - \frac{\pi}{4}), \quad (16)$$

where the prefactor σ_P^{QM} is given by Eq. (A27) in Appendix A. Details of the derivation of Eqs. (12)-(16) are presented in Appendix A. We find that Eqs. (12)-(16) (as listed in Table I) are in exact accordance with numerical results shown in Figs. 1 and 2.

It is instructive to compare the quantum-metric-induced nonlinear conductivity $\sigma_{\phi\phi\phi}^{\text{QM}}$ with nonlinear Drude conductivity $\sigma_{\phi\phi\phi}^{\text{Drude}}$ investigated previously[36]. As listed in Table I, there is the same (θ, φ) dependent relations for the same SOC in both due to their identical symmetry restrictions. However, for RSO, DSO and WSO, the signs of $\sigma_{\phi\phi\phi}^{\text{QM}}$ and $\sigma_{\phi\phi\phi}^{\text{Drude}}$ for the same SOC are opposite, which results in the compensated

contribution to the total nonlinear conductivity. For example, $\sigma_R^{\text{Drude}} = e^3 \tau^2 \alpha \Delta / (4\pi \hbar^3 \epsilon_F)$ [36] and σ_R^{QM} [Eq. (13)] have opposite signs but reveal distinct ϵ_F dependency relations. In the case of PSO, $\sigma_{\phi\phi\phi}^{\text{Drude}}$ and $\sigma_{\phi\phi\phi}^{\text{QM}}$ have the same sign but distinct ϕ dependency relations: the former is $\sin(\phi - \pi/4)$ dependent and the latter is $\sin^3(\phi - \pi/4)$ dependent. As such, it is feasible to separate different contributions from the sign of nonlinear conductivity or its ϕ dependent relations.

IV. DISCUSSION AND CONCLUSIONS

In this work, we study the magnetically tunable nonlinear transport based on the Hamiltonian model. For realistic systems, it is promising to consider the 2D material with SOC on top of a ferromagnetic or antiferromagnetic insulator. For example, an Ag_2Te monolayer with RSO on top of the Cr_2O_3 is one of the promising candidates[36, 37]. An alternative way is by applying an external magnetic field on 2D materials. The density functional theory calculations on realistic systems will be provided in the future study. Second, the similar approach can be readily generalized to three-dimensional systems. Lastly, since the polarity of the nonlinear conductivity is locked to the magnetic order parameters such as magnetization and Néel vector, measuring the magnetic control of nonlinear conductivity offers an efficient way to detect those

magnetic order parameters, which is beneficial for future devices.

In summary, using the Boltzmann transport theory, we have studied the magnetic control of nonlinear transport induced by the quantum metric in two dimensions. Our results show that the nonlinear conductivity can be significantly tuned by the direction of a field and reveals strong spatial anisotropy. We further derive the analytical formulas of the nonlinear conductivity for different SOCs, which are in exact agreement with numerical results. Our work establishes a fundamental strategy in exploring the nonlinear transport physics due to the *intrinsic* quantum geometry.

ACKNOWLEDGMENTS

This research was supported by the National Natural Science Foundation of China (Grant No. 12274102).

DATA AVAILABILITY

The data that support the findings of this article are not publicly available upon publication because it is not technically feasible and/or the cost of preparing, depositing, and hosting the data would be prohibitive within the terms of this research project. The data are available from the authors upon reasonable request.

Appendix A: Derivation of Eqs. (12)-(16)

For RSO, we have $\Omega(\mathbf{k}) = \alpha(-k_y, k_x, 0)$ and $\mathbf{h}(\mathbf{k}) = (-\alpha k_y - \Delta \hat{m}_x, \alpha k_x - \Delta \hat{m}_y, -\Delta \hat{m}_z)$. It follows from Eq. (9) that

$$G_s^{xx} = s \frac{\alpha^2(h_x^2 + h_z^2)}{4h^5}, G_s^{yy} = s \frac{\alpha^2(h_y^2 + h_z^2)}{4h^5}, G_s^{xy} = s \frac{\alpha^2 h_x h_y}{4h^5}. \quad (\text{A1})$$

In zero order, the Fermi wave number k_{Fs} can be calculated as $k_{Fs} \approx \sqrt{k_0^2 + k_R^2} - sk_R$ with $k_0 = \sqrt{2m_e \epsilon_F / \hbar^2}$ and $k_R = m_e |\alpha| / \hbar^2$. We substitute in Eq. (11) and find that

$$\begin{aligned} \sigma_{xxx}^{\text{QM}} &= -\frac{e^3}{4\pi^2 \hbar} \sum_s \int f_s \frac{\partial G_s^{xx}}{\partial k_x} d^2 k = -\frac{5\alpha^3 e^3}{16\pi^2 \hbar} \int_0^{2\pi} d\phi \int_{k_{F-}}^{k_{F+}} \left(\frac{h_y^3}{h^7} - \frac{h_y}{h^5} \right) k dk, \\ \sigma_{yyy}^{\text{QM}} &= -\frac{e^3}{4\pi^2 \hbar} \sum_s \int f_s \frac{\partial G_s^{yy}}{\partial k_y} d^2 k = -\frac{5\alpha^3 e^3}{16\pi^2 \hbar} \int_0^{2\pi} d\phi \int_{k_{F-}}^{k_{F+}} \left(\frac{h_x^3}{h^7} - \frac{h_x}{h^5} \right) k dk, \\ \sigma_{yxx}^{\text{QM}} &= -\frac{e^3}{4\pi^2 \hbar} \sum_s \int f_s \left(2 \frac{\partial G_s^{xx}}{\partial k_y} - \frac{\partial G_s^{xy}}{\partial k_x} \right) d^2 k \approx -\frac{5\alpha^3 e^3}{16\pi^2 \hbar} \int_0^{2\pi} d\phi \int_{k_{F-}}^{k_{F+}} \frac{h_x^3}{h^7} k dk, \\ \sigma_{xxy}^{\text{QM}} &= -\frac{e^3}{4\pi^2 \hbar} \sum_s \int f_s \left(\frac{3}{2} \frac{\partial G_s^{xy}}{\partial k_x} - \frac{1}{2} \frac{\partial G_s^{xx}}{\partial k_y} \right) d^2 k \approx \frac{5\alpha^3 e^3}{16\pi^2 \hbar} \int_0^{2\pi} d\phi \int_{k_{F-}}^{k_{F+}} \left(\frac{h_x}{h^5} - \frac{h_x^3}{h^7} \right) k dk, \\ \sigma_{yxy}^{\text{QM}} &= -\frac{e^3}{4\pi^2 \hbar} \sum_s \int f_s \left(\frac{3}{2} \frac{\partial G_s^{xy}}{\partial k_y} - \frac{1}{2} \frac{\partial G_s^{yy}}{\partial k_x} \right) d^2 k \approx \frac{5\alpha^3 e^3}{16\pi^2 \hbar} \int_0^{2\pi} d\phi \int_{k_{F-}}^{k_{F+}} \left(\frac{h_y^3}{h^7} - \frac{h_y}{h^5} \right) k dk, \\ \sigma_{xyy}^{\text{QM}} &= -\frac{e^3}{4\pi^2 \hbar} \sum_s \int f_s \left(2 \frac{\partial G_s^{yy}}{\partial k_x} - \frac{\partial G_s^{yx}}{\partial k_y} \right) d^2 k \approx \frac{5\alpha^3 e^3}{16\pi^2 \hbar} \int_0^{2\pi} d\phi \int_{k_{F-}}^{k_{F+}} \frac{h_y^3}{h^7} k dk. \end{aligned} \quad (\text{A2})$$

To first order in Δ , the integrals in Eq. (A2) can be calculated as

$$\begin{aligned}
& \int_0^{2\pi} d\phi \int_{k_{F-}}^{k_{F+}} \frac{h_y^3}{h^7} k dk \approx \int_0^{2\pi} d\phi \int_{k_{F-}}^{k_{F+}} (\alpha^3 k_x^3 - 3\alpha^2 k_x^2 \Delta \hat{m}_y) \left[\frac{1}{|\alpha|^7 k^6} + \frac{7\alpha\Delta}{|\alpha|^9 k^7} (\hat{m}_y \cos \phi - \hat{m}_x \sin \phi) \right] dk \\
& \approx \int_0^{2\pi} d\phi \int_{k_{F-}}^{k_{F+}} \left[\frac{\cos^3 \phi}{\alpha^3 |\alpha| k^3} + \frac{7\Delta \cos^3 \phi}{|\alpha|^5 k^4} (\hat{m}_y \cos \phi - \hat{m}_x \sin \phi) - \frac{3\Delta \hat{m}_y \cos^2 \phi}{|\alpha|^5 k^4} \right] dk \\
& = \int_0^{2\pi} \left[\frac{\cos^3 \phi}{\alpha^3 |\alpha|} \left(\frac{1}{2k_{F-}^2} - \frac{1}{2k_{F+}^2} \right) + \frac{\Delta \hat{m}_y (7 \cos^4 \phi - 3 \cos^2 \phi) - 7\Delta \hat{m}_x \cos^3 \phi \sin \phi}{|\alpha|^5} \left(\frac{1}{3k_{F-}^3} - \frac{1}{3k_{F+}^3} \right) \right] d\phi \\
& \approx \int_0^{2\pi} \left[\frac{\cos^3 \phi}{\alpha^3 |\alpha|} \left(-\frac{2k_R \sqrt{k_0^2 + k_R^2}}{k_0^4} \right) + \frac{\Delta \hat{m}_y (7 \cos^4 \phi - 3 \cos^2 \phi) - 7\Delta \hat{m}_x \cos^3 \phi \sin \phi}{|\alpha|^5} \left(-\frac{2k_R (3k_0^2 + 4k_R^2)}{3k_0^6} \right) \right] d\phi \\
& = -\frac{2k_R (3k_0^2 + 4k_R^2)}{3k_0^6} \int_0^{2\pi} \frac{\Delta \hat{m}_y (7 \cos^4 \phi - 3 \cos^2 \phi)}{|\alpha|^5} d\phi \\
& = -\frac{3\pi (3\hbar^2 \epsilon_F + 2m_e \alpha^2) \Delta}{8m_e \alpha^4 \epsilon_F^3} \sin \theta \sin \varphi,
\end{aligned} \tag{A3}$$

and

$$\begin{aligned}
& \int_0^{2\pi} d\phi \int_{k_{F-}}^{k_{F+}} \frac{h_y}{h^5} k dk \approx \int_0^{2\pi} d\phi \int_{k_{F-}}^{k_{F+}} (\alpha k_x - \Delta \hat{m}_y) \left[\frac{1}{|\alpha|^5 k^4} + \frac{5\alpha\Delta}{|\alpha|^7 k^5} (\hat{m}_y \cos \phi - \hat{m}_x \sin \phi) \right] dk \\
& \approx \int_0^{2\pi} d\phi \int_{k_{F-}}^{k_{F+}} \left[\frac{\alpha \cos \phi}{|\alpha|^5 k^3} + \frac{5\Delta \cos \phi}{|\alpha|^5 k^4} (\hat{m}_y \cos \phi - \hat{m}_x \sin \phi) - \frac{\Delta \hat{m}_y}{|\alpha|^5 k^4} \right] dk \\
& = \int_0^{2\pi} \left[\frac{\alpha \cos \phi}{|\alpha|^5} \left(\frac{1}{2k_{F-}^2} - \frac{1}{2k_{F+}^2} \right) + \frac{\Delta}{|\alpha|^5} (5\hat{m}_y \cos^2 \phi - 5\hat{m}_x \cos \phi \sin \phi - \hat{m}_y) \left(\frac{1}{3k_{F-}^3} - \frac{1}{3k_{F+}^3} \right) \right] d\phi \\
& \approx \int_0^{2\pi} \left[\frac{\alpha \cos \phi}{|\alpha|^5} \left(-\frac{2k_R \sqrt{k_0^2 + k_R^2}}{k_0^4} \right) + \frac{\Delta}{|\alpha|^5} (5\hat{m}_y \cos^2 \phi - 5\hat{m}_x \cos \phi \sin \phi - \hat{m}_y) \left(-\frac{2k_R (3k_0^2 + 4k_R^2)}{3k_0^6} \right) \right] d\phi \\
& = -\frac{2k_R (3k_0^2 + 4k_R^2)}{3k_0^6} \int_0^{2\pi} \left[\frac{\Delta \hat{m}_y}{|\alpha|^5} (5 \cos^2 \phi - 1) \right] d\phi \\
& = -\frac{\pi (3\hbar^2 \epsilon_F + 2m_e \alpha^2) \Delta}{2m_e \alpha^4 \epsilon_F^3} \sin \theta \sin \varphi,
\end{aligned} \tag{A4}$$

and

$$\begin{aligned}
& \int_0^{2\pi} d\phi \int_{k_{F-}}^{k_{F+}} \frac{h_x}{h^5} k dk \approx - \int_0^{2\pi} d\phi \int_{k_{F-}}^{k_{F+}} (\alpha k_y + \Delta \hat{m}_x) \left[\frac{1}{|\alpha|^5 k^4} + \frac{5\alpha\Delta}{|\alpha|^7 k^5} (\hat{m}_y \cos \phi - \hat{m}_x \sin \phi) \right] dk \\
& \approx - \int_0^{2\pi} d\phi \int_{k_{F-}}^{k_{F+}} \left[\frac{\alpha \sin \phi}{|\alpha|^5 k^3} + \frac{5\Delta \sin \phi}{|\alpha|^5 k^4} (\hat{m}_y \cos \phi - \hat{m}_x \sin \phi) + \frac{\Delta \hat{m}_x}{|\alpha|^5 k^4} \right] dk \\
& = - \int_0^{2\pi} \left[\frac{\alpha \sin \phi}{|\alpha|^5} \left(\frac{1}{2k_{F-}^2} - \frac{1}{2k_{F+}^2} \right) + \frac{\Delta}{|\alpha|^5} (5\hat{m}_y \cos \phi \sin \phi - 5\hat{m}_x \sin^2 \phi + \hat{m}_x) \left(\frac{1}{3k_{F-}^3} - \frac{1}{3k_{F+}^3} \right) \right] d\phi \\
& \approx -\frac{2k_R (3k_0^2 + 4k_R^2)}{3k_0^6} \int_0^{2\pi} \left[\frac{\Delta \hat{m}_x}{|\alpha|^5} (5 \sin^2 \phi - 1) \right] d\phi \\
& = -\frac{\pi (3\hbar^2 \epsilon_F + 2m_e \alpha^2) \Delta}{2m_e \alpha^4 \epsilon_F^3} \sin \theta \cos \varphi,
\end{aligned} \tag{A5}$$

and

$$\begin{aligned}
& \int_0^{2\pi} d\phi \int_{k_{F-}}^{k_{F+}} \frac{h_x^3}{h^7} k dk \approx - \int_0^{2\pi} d\phi \int_{k_{F-}}^{k_{F+}} (\alpha^3 k_y^3 + 3\alpha^2 k_y^2 \Delta \hat{m}_x) \left[\frac{1}{|\alpha|^7 k^6} + \frac{7\alpha\Delta}{|\alpha|^9 k^7} (\hat{m}_y \cos \phi - \hat{m}_x \sin \phi) \right] dk \\
& \approx - \int_0^{2\pi} d\phi \int_{k_{F-}}^{k_{F+}} \left[\frac{\sin^3 \phi}{\alpha^3 |\alpha| k^3} + \frac{7\Delta \sin^3 \phi}{|\alpha|^5 k^4} (\hat{m}_y \cos \phi - \hat{m}_x \sin \phi) + \frac{3\Delta \hat{m}_x \sin^2 \phi}{|\alpha|^5 k^4} \right] dk \\
& \approx - \frac{2k_R(3k_0^2 + 4k_R^2)}{3k_0^6} \int_0^{2\pi} \frac{\Delta \hat{m}_x (7 \sin^4 \phi - 3 \sin^2 \phi)}{|\alpha|^5} d\phi \\
& = - \frac{3\pi(3\hbar^2 \epsilon_F + 2m_e \alpha^2) \Delta}{8m_e \alpha^4 \epsilon_F^3} \sin \theta \cos \varphi.
\end{aligned} \tag{A6}$$

Substitution of Eqs. (A3)-(A6) in Eq. (A2) yields

$$\begin{aligned}
\sigma_{xxx}^{\text{QM}} &= \sigma_R^{\text{QM}} \sin \theta \sin \varphi, \quad \sigma_{yyy}^{\text{QM}} = -\sigma_R^{\text{QM}} \sin \theta \cos \varphi, \quad \sigma_{yxx}^{\text{QM}} = -3\sigma_R^{\text{QM}} \sin \theta \cos \varphi, \\
\sigma_{xxy}^{\text{QM}} &= \sigma_R^{\text{QM}} \sin \theta \cos \varphi, \quad \sigma_{xyy}^{\text{QM}} = -\sigma_R^{\text{QM}} \sin \theta \sin \varphi, \quad \sigma_{xyy}^{\text{QM}} = 3\sigma_R^{\text{QM}} \sin \theta \sin \varphi, \\
\sigma_R^{\text{QM}} &\equiv - \frac{5e^3(3\hbar^2 \epsilon_F + 2m_e \alpha^2) \Delta}{128\pi \hbar m_e \alpha \epsilon_F^3}.
\end{aligned} \tag{A7}$$

We substitute in Eq. (10) and find that

$$\begin{aligned}
\sigma_{\phi\phi\phi}^{\text{QM}} &= \sigma_{xxx}^{\text{QM}} \cos^3 \phi + \sigma_{yyy}^{\text{QM}} \sin^3 \phi + (\sigma_{xyy}^{\text{QM}} + 2\sigma_{xxy}^{\text{QM}}) \sin^2 \phi \cos \phi + (\sigma_{yxx}^{\text{QM}} + 2\sigma_{xxy}^{\text{QM}}) \sin \phi \cos^2 \phi \\
&= \sigma_{xxx}^{\text{QM}} \cos^3 \phi + \sigma_{yyy}^{\text{QM}} \sin^3 \phi + (3\sigma_{xxx}^{\text{QM}} - 2\sigma_{xxy}^{\text{QM}}) \sin^2 \phi \cos \phi + (3\sigma_{yyy}^{\text{QM}} - 2\sigma_{xyy}^{\text{QM}}) \sin \phi \cos^2 \phi \\
&= \sigma_{xxx}^{\text{QM}} \cos \phi + \sigma_{yyy}^{\text{QM}} \sin \phi = \sigma_R^{\text{QM}} \sin \theta \sin(\varphi - \phi).
\end{aligned} \tag{A8}$$

The above procedures to derive $\sigma_{\phi\phi\phi}^{\text{QM}}$ can be readily generalized to other SOCs. For DSO, we have $\mathbf{h}(\mathbf{k}) = (\beta k_x - \Delta \hat{m}_x, -\beta k_y - \Delta \hat{m}_y, -\Delta \hat{m}_z)$ and

$$G_s^{xx} = s \frac{\beta^2(h_y^2 + h_z^2)}{4h^5}, \quad G_s^{yy} = s \frac{\beta^2(h_x^2 + h_z^2)}{4h^5}, \quad G_s^{xy} = s \frac{\beta^2 h_x h_y}{4h^5}. \tag{A9}$$

We substitute in Eq. (11) and find that

$$\begin{aligned}
\sigma_{xxx}^{\text{QM}} &= - \frac{e^3}{4\pi^2 \hbar} \sum_s \int f_s \frac{\partial G_s^{xx}}{\partial k_x} d^2 k = - \frac{5\beta^3 e^3}{16\pi^2 \hbar} \int_0^{2\pi} d\phi \int_{k_{F-}}^{k_{F+}} \left(\frac{h_x^3}{h^7} - \frac{h_x}{h^5} \right) k dk, \\
\sigma_{yyy}^{\text{QM}} &= - \frac{e^3}{4\pi^2 \hbar} \sum_s \int f_s \frac{\partial G_s^{yy}}{\partial k_y} d^2 k = - \frac{5\beta^3 e^3}{16\pi^2 \hbar} \int_0^{2\pi} d\phi \int_{k_{F-}}^{k_{F+}} \left(\frac{h_y}{h^5} - \frac{h_y^3}{h^7} \right) k dk, \\
\sigma_{yxx}^{\text{QM}} &= - \frac{e^3}{4\pi^2 \hbar} \sum_s \int f_s \left(2 \frac{\partial G_s^{xx}}{\partial k_y} - \frac{\partial G_s^{xy}}{\partial k_x} \right) d^2 k \approx - \frac{5\beta^3 e^3}{16\pi^2 \hbar} \int_0^{2\pi} d\phi \int_{k_{F-}}^{k_{F+}} \frac{h_y^3}{h^7} k dk, \\
\sigma_{xxy}^{\text{QM}} &= - \frac{e^3}{4\pi^2 \hbar} \sum_s \int f_s \left(\frac{3}{2} \frac{\partial G_s^{xy}}{\partial k_x} - \frac{1}{2} \frac{\partial G_s^{xx}}{\partial k_y} \right) d^2 k \approx \frac{5\beta^3 e^3}{16\pi^2 \hbar} \int_0^{2\pi} d\phi \int_{k_{F-}}^{k_{F+}} \left(\frac{h_y}{h^5} - \frac{h_y^3}{h^7} \right) k dk, \\
\sigma_{xyy}^{\text{QM}} &= - \frac{e^3}{4\pi^2 \hbar} \sum_s \int f_s \left(\frac{3}{2} \frac{\partial G_s^{xy}}{\partial k_y} - \frac{1}{2} \frac{\partial G_s^{yy}}{\partial k_x} \right) d^2 k \approx \frac{5\beta^3 e^3}{16\pi^2 \hbar} \int_0^{2\pi} d\phi \int_{k_{F-}}^{k_{F+}} \left(\frac{h_x}{h^5} - \frac{h_x}{h^7} \right) k dk, \\
\sigma_{xyy}^{\text{QM}} &= - \frac{e^3}{4\pi^2 \hbar} \sum_s \int f_s \left(2 \frac{\partial G_s^{yy}}{\partial k_x} - \frac{\partial G_s^{yx}}{\partial k_y} \right) d^2 k \approx \frac{5\beta^3 e^3}{16\pi^2 \hbar} \int_0^{2\pi} d\phi \int_{k_{F-}}^{k_{F+}} \frac{h_x^3}{h^7} k dk.
\end{aligned} \tag{A10}$$

To first order in Δ , we have

$$\begin{aligned}
& \int_0^{2\pi} d\phi \int_{k_{F-}}^{k_{F+}} \frac{h_x^3}{h^7} k dk \approx \int_0^{2\pi} d\phi \int_{k_{F-}}^{k_{F+}} (\beta^3 k_x^3 - 3\beta^2 k_x^2 \Delta \hat{m}_x) \left[\frac{1}{|\beta|^7 k^6} + \frac{7\beta\Delta}{|\beta|^9 k^7} (\hat{m}_x \cos \phi - \hat{m}_y \sin \phi) \right] dk \\
& \approx \int_0^{2\pi} d\phi \int_{k_{F-}}^{k_{F+}} \left[\frac{\cos^3 \phi}{\beta^3 |\beta| k^3} + \frac{7\Delta \cos^3 \phi}{|\beta|^5 k^4} (\hat{m}_x \cos \phi - \hat{m}_y \sin \phi) - \frac{3\Delta \hat{m}_x \cos^2 \phi}{|\beta|^5 k^4} \right] dk \\
& = \int_0^{2\pi} \left[\frac{\cos^3 \phi}{\beta^3 |\beta|} \left(\frac{1}{2k_{F-}^2} - \frac{1}{2k_{F+}^2} \right) + \frac{\Delta \hat{m}_x (7 \cos^4 \phi - 3 \cos^2 \phi) - 7\Delta \hat{m}_y \cos^3 \phi \sin \phi}{|\beta|^5} \left(\frac{1}{3k_{F-}^3} - \frac{1}{3k_{F+}^3} \right) \right] d\phi \\
& \approx -\frac{2k_D (3k_0^2 + 4k_D^2)}{3k_0^6} \int_0^{2\pi} \frac{\Delta \hat{m}_x (7 \cos^4 \phi - 3 \cos^2 \phi)}{|\beta|^5} d\phi \\
& = -\frac{3\pi (3\hbar^2 \epsilon_F + 2m_e \beta^2) \Delta}{8m_e \beta^4 \epsilon_F^3} \sin \theta \cos \varphi,
\end{aligned} \tag{A11}$$

and

$$\begin{aligned}
& \int_0^{2\pi} d\phi \int_{k_{F-}}^{k_{F+}} \frac{h_x}{h^5} k dk \approx \int_0^{2\pi} d\phi \int_{k_{F-}}^{k_{F+}} (\beta k_x - \Delta \hat{m}_x) \left[\frac{1}{|\beta|^5 k^4} + \frac{5\beta\Delta}{|\beta|^7 k^5} (\hat{m}_x \cos \phi - \hat{m}_y \sin \phi) \right] dk \\
& \approx \int_0^{2\pi} d\phi \int_{k_{F-}}^{k_{F+}} \left[\frac{\beta \cos \phi}{|\beta|^5 k^3} + \frac{5\Delta \cos \phi}{|\beta|^5 k^4} (\hat{m}_x \cos \phi - \hat{m}_y \sin \phi) - \frac{\Delta \hat{m}_x}{|\beta|^5 k^4} \right] dk \\
& = \int_0^{2\pi} \left[\frac{\beta \cos \phi}{|\beta|^5} \left(\frac{1}{2k_{F-}^2} - \frac{1}{2k_{F+}^2} \right) + \frac{\Delta}{|\beta|^5} (5\hat{m}_x \cos^2 \phi - 5\hat{m}_y \cos \phi \sin \phi - \hat{m}_x) \left(\frac{1}{3k_{F-}^3} - \frac{1}{3k_{F+}^3} \right) \right] d\phi \\
& \approx -\frac{2k_D (3k_0^2 + 4k_D^2)}{3k_0^6} \int_0^{2\pi} \left[\frac{\Delta \hat{m}_x}{|\beta|^5} (5 \cos^2 \phi - 1) \right] d\phi \\
& = -\frac{\pi (3\hbar^2 \epsilon_F + 2m_e \beta^2) \Delta}{2m_e \beta^4 \epsilon_F^3} \sin \theta \cos \varphi,
\end{aligned} \tag{A12}$$

and

$$\begin{aligned}
& \int_0^{2\pi} d\phi \int_{k_{F-}}^{k_{F+}} \frac{h_y}{h^5} k dk \approx \int_0^{2\pi} d\phi \int_{k_{F-}}^{k_{F+}} (-\beta k_y - \Delta \hat{m}_y) \left[\frac{1}{|\beta|^5 k^4} + \frac{5\beta\Delta}{|\beta|^7 k^5} (\hat{m}_x \cos \phi - \hat{m}_y \sin \phi) \right] dk \\
& \approx -\int_0^{2\pi} d\phi \int_{k_{F-}}^{k_{F+}} \left[\frac{\beta \sin \phi}{|\beta|^5 k^3} + \frac{5\Delta \sin \phi}{|\beta|^5 k^4} (\hat{m}_x \cos \phi - \hat{m}_y \sin \phi) + \frac{\Delta \hat{m}_y}{|\beta|^5 k^4} \right] dk \\
& = -\int_0^{2\pi} \left[\frac{\beta \sin \phi}{|\beta|^5} \left(\frac{1}{2k_{F-}^2} - \frac{1}{2k_{F+}^2} \right) + \frac{\Delta}{|\beta|^5} (5\hat{m}_x \cos \phi \sin \phi - 5\hat{m}_y \sin^2 \phi + \hat{m}_y) \left(\frac{1}{3k_{F-}^3} - \frac{1}{3k_{F+}^3} \right) \right] d\phi \\
& \approx -\frac{2k_D (3k_0^2 + 4k_D^2)}{3k_0^6} \int_0^{2\pi} \left[\frac{\Delta \hat{m}_y}{|\beta|^5} (5 \sin^2 \phi - 1) \right] d\phi \\
& = -\frac{\pi (3\hbar^2 \epsilon_F + 2m_e \beta^2) \Delta}{2m_e \beta^4 \epsilon_F^3} \sin \theta \sin \varphi,
\end{aligned} \tag{A13}$$

and

$$\begin{aligned}
& \int_0^{2\pi} d\phi \int_{k_{F-}}^{k_{F+}} \frac{h_y^3}{h^7} k dk \approx -\int_0^{2\pi} d\phi \int_{k_{F-}}^{k_{F+}} (\beta^3 k_y^3 + 3\beta^2 k_y^2 \Delta \hat{m}_y) \left[\frac{1}{|\beta|^7 k^6} + \frac{7\beta\Delta}{|\beta|^9 k^7} (\hat{m}_x \cos \phi - \hat{m}_y \sin \phi) \right] dk \\
& \approx -\int_0^{2\pi} d\phi \int_{k_{F-}}^{k_{F+}} \left[\frac{\sin^3 \phi}{\beta^3 |\beta| k^3} + \frac{7\Delta \sin^3 \phi}{|\beta|^5 k^4} (\hat{m}_x \cos \phi - \hat{m}_y \sin \phi) + \frac{3\Delta \hat{m}_y \sin^2 \phi}{|\beta|^5 k^4} \right] dk \\
& \approx -\frac{2k_D (3k_0^2 + 4k_D^2)}{3k_0^6} \int_0^{2\pi} \frac{\Delta \hat{m}_y (7 \sin^4 \phi - 3 \sin^2 \phi)}{|\beta|^5} d\phi \\
& = -\frac{3\pi (3\hbar^2 \epsilon_F + 2m_e \beta^2) \Delta}{8m_e \beta^4 \epsilon_F^3} \sin \theta \sin \varphi.
\end{aligned} \tag{A14}$$

with $k_0 = \sqrt{2m_e\epsilon_F/\hbar^2}$ and $k_D = m_e|\beta|/\hbar^2$. Substitution of Eqs. (A11)-(A14) in Eq. (A10) yields

$$\begin{aligned}\sigma_{xxx}^{\text{QM}} &= \sigma_D^{\text{QM}} \sin \theta \cos \varphi, \sigma_{yyy}^{\text{QM}} = -\sigma_D^{\text{QM}} \sin \theta \sin \varphi, \sigma_{yxx}^{\text{QM}} = -3\sigma_D^{\text{QM}} \sin \theta \sin \varphi, \\ \sigma_{xxy}^{\text{QM}} &= \sigma_D^{\text{QM}} \sin \theta \sin \varphi, \sigma_{yxy}^{\text{QM}} = -\sigma_D^{\text{QM}} \sin \theta \cos \varphi, \sigma_{xyy}^{\text{QM}} = 3\sigma_D^{\text{QM}} \sin \theta \cos \varphi, \\ \sigma_D^{\text{QM}} &\equiv -\frac{5e^3(3\hbar^2\epsilon_F + 2m_e\beta^2)\Delta}{128\pi\hbar m_e\beta\epsilon_F^3}.\end{aligned}\quad (\text{A15})$$

We substitute in Eq. (10) and find that

$$\begin{aligned}\sigma_{\phi\phi\phi}^{\text{QM}} &= \sigma_{xxx}^{\text{QM}} \cos^3 \phi + \sigma_{yyy}^{\text{QM}} \sin^3 \phi + (\sigma_{xyy}^{\text{QM}} + 2\sigma_{yxy}^{\text{QM}}) \sin^2 \phi \cos \phi + (\sigma_{yxx}^{\text{QM}} + 2\sigma_{xxy}^{\text{QM}}) \sin \phi \cos^2 \phi \\ &= \sigma_{xxx}^{\text{QM}} \cos^3 \phi + \sigma_{yyy}^{\text{QM}} \sin^3 \phi + (3\sigma_{xxx}^{\text{QM}} - 2\sigma_{xxy}^{\text{QM}}) \sin^2 \phi \cos \phi + (3\sigma_{yyy}^{\text{QM}} - 2\sigma_{xyy}^{\text{QM}}) \sin \phi \cos^2 \phi \\ &= \sigma_{xxx}^{\text{QM}} \cos \phi + \sigma_{yyy}^{\text{QM}} \sin \phi = \sigma_D^{\text{QM}} \sin \theta \cos(\varphi + \phi).\end{aligned}\quad (\text{A16})$$

For WSO, we have $\mathbf{h}(\mathbf{k}) = (\gamma k_x - \Delta \hat{m}_x, \gamma k_y - \Delta \hat{m}_y, -\Delta \hat{m}_z)$ and

$$G_s^{xx} = s \frac{\gamma^2(h_y^2 + h_z^2)}{4\hbar^5}, G_s^{yy} = s \frac{\gamma^2(h_x^2 + h_z^2)}{4\hbar^5}, G_s^{xy} = -s \frac{\gamma^2 h_x h_y}{4\hbar^5}. \quad (\text{A17})$$

We substitute in Eq. (11) and find that

$$\begin{aligned}\sigma_{xxx}^{\text{QM}} &= -\frac{e^3}{4\pi^2\hbar} \sum_s \int f_s \frac{\partial G_s^{xx}}{\partial k_x} d^2k = -\frac{5\gamma^3 e^3}{16\pi^2\hbar} \int_0^{2\pi} d\phi \int_{k_{F-}}^{k_{F+}} \left(\frac{h_x^3}{\hbar^7} - \frac{h_x}{\hbar^5}\right) k dk, \\ \sigma_{yyy}^{\text{QM}} &= -\frac{e^3}{4\pi^2\hbar} \sum_s \int f_s \frac{\partial G_s^{yy}}{\partial k_y} d^2k = -\frac{5\gamma^3 e^3}{16\pi^2\hbar} \int_0^{2\pi} d\phi \int_{k_{F-}}^{k_{F+}} \left(\frac{h_y^3}{\hbar^7} - \frac{h_y}{\hbar^5}\right) k dk, \\ \sigma_{yxx}^{\text{QM}} &= -\frac{e^3}{4\pi^2\hbar} \sum_s \int f_s \left(2 \frac{\partial G_s^{xx}}{\partial k_y} - \frac{\partial G_s^{xy}}{\partial k_x}\right) d^2k \approx \frac{5\gamma^3 e^3}{16\pi^2\hbar} \int_0^{2\pi} d\phi \int_{k_{F-}}^{k_{F+}} \frac{h_y^3}{\hbar^7} k dk, \\ \sigma_{xxy}^{\text{QM}} &= -\frac{e^3}{4\pi^2\hbar} \sum_s \int f_s \left(\frac{3}{2} \frac{\partial G_s^{xy}}{\partial k_x} - \frac{1}{2} \frac{\partial G_s^{yy}}{\partial k_y}\right) d^2k \approx \frac{5\gamma^3 e^3}{16\pi^2\hbar} \int_0^{2\pi} d\phi \int_{k_{F-}}^{k_{F+}} \left(\frac{h_y^3}{\hbar^7} - \frac{h_y}{\hbar^5}\right) k dk, \\ \sigma_{xyy}^{\text{QM}} &= -\frac{e^3}{4\pi^2\hbar} \sum_s \int f_s \left(\frac{3}{2} \frac{\partial G_s^{xy}}{\partial k_y} - \frac{1}{2} \frac{\partial G_s^{yy}}{\partial k_x}\right) d^2k \approx \frac{5\gamma^3 e^3}{16\pi^2\hbar} \int_0^{2\pi} d\phi \int_{k_{F-}}^{k_{F+}} \left(\frac{h_x^3}{\hbar^7} - \frac{h_x}{\hbar^5}\right) k dk, \\ \sigma_{xyy}^{\text{QM}} &= -\frac{e^3}{4\pi^2\hbar} \sum_s \int f_s \left(2 \frac{\partial G_s^{yy}}{\partial k_x} - \frac{\partial G_s^{yx}}{\partial k_y}\right) d^2k \approx \frac{5\gamma^3 e^3}{16\pi^2\hbar} \int_0^{2\pi} d\phi \int_{k_{F-}}^{k_{F+}} \frac{h_x^3}{\hbar^7} k dk.\end{aligned}\quad (\text{A18})$$

To first order in Δ , we have

$$\begin{aligned}\int_0^{2\pi} d\phi \int_{k_{F-}}^{k_{F+}} \frac{h_x^3}{\hbar^7} k dk &\approx \int_0^{2\pi} d\phi \int_{k_{F-}}^{k_{F+}} (\gamma^3 k_x^3 - 3\gamma^2 k_x^2 \Delta \hat{m}_x) \left[\frac{1}{|\gamma|^7 k^6} + \frac{7\gamma\Delta}{|\gamma|^9 k^7} (\hat{m}_x \cos \phi + \hat{m}_y \sin \phi)\right] dk \\ &\approx \int_0^{2\pi} d\phi \int_{k_{F-}}^{k_{F+}} \left[\frac{\cos^3 \phi}{\gamma^3 |\gamma| k^3} + \frac{7\Delta \cos^3 \phi}{|\gamma|^5 k^4} (\hat{m}_x \cos \phi + \hat{m}_y \sin \phi) - \frac{3\Delta \hat{m}_x \cos^2 \phi}{|\gamma|^5 k^4}\right] dk \\ &= \int_0^{2\pi} \left[\frac{\cos^3 \phi}{\gamma^3 |\gamma|} \left(\frac{1}{2k_{F-}^2} - \frac{1}{2k_{F+}^2}\right) + \frac{\Delta \hat{m}_x (7 \cos^4 \phi - 3 \cos^2 \phi) + 7\Delta \hat{m}_y \cos^3 \phi \sin \phi}{|\gamma|^5} \left(\frac{1}{3k_{F-}^3} - \frac{1}{3k_{F+}^3}\right)\right] d\phi \\ &\approx -\frac{2k_W(3k_0^2 + 4k_W^2)}{3k_0^6} \int_0^{2\pi} \frac{\Delta \hat{m}_x (7 \cos^4 \phi - 3 \cos^2 \phi)}{|\gamma|^5} d\phi \\ &= -\frac{3\pi(3\hbar^2\epsilon_F + 2m_e\gamma^2)\Delta}{8m_e\gamma^4\epsilon_F^3} \sin \theta \cos \varphi,\end{aligned}\quad (\text{A19})$$

and

$$\begin{aligned}
\int_0^{2\pi} d\phi \int_{k_{F_-}}^{k_{F+}} \frac{h_x}{h^5} k dk &\approx \int_0^{2\pi} d\phi \int_{k_{F_-}}^{k_{F+}} (\gamma k_x - \Delta \hat{m}_x) \left[\frac{1}{|\gamma|^5 k^4} + \frac{5\gamma\Delta}{|\gamma|^7 k^5} (\hat{m}_x \cos \phi + \hat{m}_y \sin \phi) \right] dk \\
&\approx \int_0^{2\pi} d\phi \int_{k_{F_-}}^{k_{F+}} \left[\frac{\gamma \cos \phi}{|\gamma|^5 k^3} + \frac{5\Delta \cos \phi}{|\gamma|^5 k^4} (\hat{m}_x \cos \phi + \hat{m}_y \sin \phi) - \frac{\Delta \hat{m}_x}{|\gamma|^5 k^4} \right] dk \\
&= \int_0^{2\pi} \left[\frac{\gamma \cos \phi}{|\gamma|^5} \left(\frac{1}{2k_{F_-}^2} - \frac{1}{2k_{F+}^2} \right) + \frac{\Delta}{|\gamma|^5} (5\hat{m}_x \cos^2 \phi + 5\hat{m}_y \cos \phi \sin \phi - \hat{m}_x) \left(\frac{1}{3k_{F_-}^3} - \frac{1}{3k_{F+}^3} \right) \right] d\phi \\
&\approx -\frac{2k_W(3k_0^2 + 4k_W^2)}{3k_0^6} \int_0^{2\pi} \left[\frac{\Delta \hat{m}_x}{|\gamma|^5} (5 \cos^2 \phi - 1) \right] d\phi \\
&= -\frac{\pi(3\hbar^2\epsilon_F + 2m_e\gamma^2)\Delta}{2m_e\gamma^4\epsilon_F^3} \sin \theta \cos \varphi,
\end{aligned} \tag{A20}$$

and

$$\begin{aligned}
\int_0^{2\pi} d\phi \int_{k_{F_-}}^{k_{F+}} \frac{h_y}{h^5} k dk &\approx \int_0^{2\pi} d\phi \int_{k_{F_-}}^{k_{F+}} (\gamma k_y - \Delta \hat{m}_y) \left[\frac{1}{|\gamma|^5 k^4} + \frac{5\gamma\Delta}{|\gamma|^7 k^5} (\hat{m}_x \cos \phi + \hat{m}_y \sin \phi) \right] dk \\
&\approx \int_0^{2\pi} d\phi \int_{k_{F_-}}^{k_{F+}} \left[\frac{\gamma \sin \phi}{|\gamma|^5 k^3} + \frac{5\Delta \sin \phi}{|\gamma|^5 k^4} (\hat{m}_x \cos \phi + \hat{m}_y \sin \phi) - \frac{\Delta \hat{m}_y}{|\gamma|^5 k^4} \right] dk \\
&= \int_0^{2\pi} \left[\frac{\gamma \sin \phi}{|\gamma|^5} \left(\frac{1}{2k_{F_-}^2} - \frac{1}{2k_{F+}^2} \right) + \frac{\Delta}{|\gamma|^5} (5\hat{m}_x \cos \phi \sin \phi + 5\hat{m}_y \sin^2 \phi - \hat{m}_y) \left(\frac{1}{3k_{F_-}^3} - \frac{1}{3k_{F+}^3} \right) \right] d\phi \\
&\approx -\frac{2k_W(3k_0^2 + 4k_W^2)}{3k_0^6} \int_0^{2\pi} \left[\frac{\Delta \hat{m}_y}{|\gamma|^5} (5 \sin^2 \phi - 1) \right] d\phi \\
&= -\frac{\pi(3\hbar^2\epsilon_F + 2m_e\gamma^2)\Delta}{2m_e\gamma^4\epsilon_F^3} \sin \theta \sin \varphi,
\end{aligned} \tag{A21}$$

and

$$\begin{aligned}
\int_0^{2\pi} d\phi \int_{k_{F_-}}^{k_{F+}} \frac{h_y^3}{h^7} k dk &\approx \int_0^{2\pi} d\phi \int_{k_{F_-}}^{k_{F+}} (\gamma^3 k_y^3 - 3\gamma^2 k_y^2 \Delta \hat{m}_y) \left[\frac{1}{|\gamma|^7 k^6} + \frac{7\gamma\Delta}{|\gamma|^9 k^7} (\hat{m}_x \cos \phi + \hat{m}_y \sin \phi) \right] dk \\
&\approx \int_0^{2\pi} d\phi \int_{k_{F_-}}^{k_{F+}} \left[\frac{\sin^3 \phi}{\gamma^3 |\gamma| k^3} + \frac{7\Delta \sin^3 \phi}{|\gamma|^5 k^4} (\hat{m}_x \cos \phi + \hat{m}_y \sin \phi) - \frac{3\Delta \hat{m}_y \sin^2 \phi}{|\gamma|^5 k^4} \right] dk \\
&\approx -\frac{2k_W(3k_0^2 + 4k_W^2)}{3k_0^6} \int_0^{2\pi} \frac{\Delta \hat{m}_y (7 \sin^4 \phi - 3 \sin^2 \phi)}{|\gamma|^5} d\phi \\
&= -\frac{3\pi(3\hbar^2\epsilon_F + 2m_e\gamma^2)\Delta}{8m_e\gamma^4\epsilon_F^3} \sin \theta \sin \varphi.
\end{aligned} \tag{A22}$$

with $k_0 = \sqrt{2m_e\epsilon_F/\hbar^2}$ and $k_W = m_e|\gamma|/\hbar^2$. Substitution of Eqs. (A19)-(A22) in Eq. (A18) yields

$$\begin{aligned}
\sigma_{xxx}^{\text{QM}} &= \sigma_W^{\text{QM}} \sin \theta \cos \varphi, \quad \sigma_{yyy}^{\text{QM}} = \sigma_W^{\text{QM}} \sin \theta \sin \varphi, \quad \sigma_{yxx}^{\text{QM}} = 3\sigma_W^{\text{QM}} \sin \theta \sin \varphi, \\
\sigma_{xxy}^{\text{QM}} &= -\sigma_W^{\text{QM}} \sin \theta \sin \varphi, \quad \sigma_{xyy}^{\text{QM}} = -\sigma_W^{\text{QM}} \sin \theta \cos \varphi, \quad \sigma_{xyy}^{\text{QM}} = 3\sigma_W^{\text{QM}} \sin \theta \cos \varphi, \\
\sigma_W^{\text{QM}} &\equiv -\frac{5e^3(3\hbar^2\epsilon_F + 2m_e\gamma^2)\Delta}{128\pi\hbar m_e\gamma\epsilon_F^3}.
\end{aligned} \tag{A23}$$

We substitute in Eq. (10) and find that

$$\sigma_{\phi\phi\phi}^{\text{QM}} = \sigma_{xxx}^{\text{QM}} \cos \phi + \sigma_{yyy}^{\text{QM}} \sin \phi = \sigma_W^{\text{QM}} \sin \theta \cos(\varphi - \phi). \tag{A24}$$

For PSO, we have $\mathbf{h}(\mathbf{k}) = (\delta(k_x - k_y) - \Delta \hat{m}_x, \delta(k_x - k_y) - \Delta \hat{m}_y, -\Delta \hat{m}_z)$ and

$$G_s^{xx} = G_s^{yy} = -G_s^{xy} = s\delta^2 \frac{2h^2 - (h_x + h_y)^2}{4h^5}. \tag{A25}$$

We substitute in Eq. (11) and find that

$$\begin{aligned}
\sigma_{xxx}^{\text{QM}} &= -\frac{e^3}{4\pi^2\hbar} \sum_s \int f_s \frac{\partial G_s^{xx}}{\partial k_x} d^2k = -\frac{5\delta^3 e^3}{16\pi^2\hbar} \int_0^{2\pi} d\phi \int_{k_F-}^{k_F+} \left[\frac{(h_x + h_y)^3}{h^7} - \frac{2(h_x + h_y)}{h^5} \right] k dk, \\
\sigma_{yyy}^{\text{QM}} &= -\frac{e^3}{4\pi^2\hbar} \sum_s \int f_s \frac{\partial G_s^{yy}}{\partial k_y} d^2k = -\sigma_{xxx}^{\text{QM}}, \\
\sigma_{yxx}^{\text{QM}} &= -\frac{e^3}{4\pi^2\hbar} \sum_s \int f_s \left(2 \frac{\partial G_s^{xx}}{\partial k_y} - \frac{\partial G_s^{xy}}{\partial k_x} \right) d^2k = -\sigma_{xxx}^{\text{QM}}, \\
\sigma_{xxy}^{\text{QM}} &= -\frac{e^3}{4\pi^2\hbar} \sum_s \int f_s \left(\frac{3}{2} \frac{\partial G_s^{xy}}{\partial k_x} - \frac{1}{2} \frac{\partial G_s^{xx}}{\partial k_y} \right) d^2k = -\sigma_{xxx}^{\text{QM}}, \\
\sigma_{yxy}^{\text{QM}} &= -\frac{e^3}{4\pi^2\hbar} \sum_s \int f_s \left(\frac{3}{2} \frac{\partial G_s^{xy}}{\partial k_y} - \frac{1}{2} \frac{\partial G_s^{yy}}{\partial k_x} \right) d^2k = \sigma_{xxx}^{\text{QM}}, \\
\sigma_{xyy}^{\text{QM}} &= -\frac{e^3}{4\pi^2\hbar} \sum_s \int f_s \left(2 \frac{\partial G_s^{yy}}{\partial k_x} - \frac{\partial G_s^{yx}}{\partial k_y} \right) d^2k = \sigma_{xxx}^{\text{QM}}.
\end{aligned} \tag{A26}$$

It is seen that only σ_{xxx}^{QM} needs to be calculated. Moreover, from the Fig. 2(f), the integrand $\partial G_s^{xx}/\partial k_x$ is pronounced around $k_x = k_y$. Thus, we have

$$\begin{aligned}
\sigma_{xxx}^{\text{QM}} &= -\frac{5\delta^3 e^3}{16\pi^2\hbar} \int_0^{2\pi} d\phi \int_{k_F-}^{k_F+} \left[\frac{(h_x + h_y)^3}{h^7} - \frac{2(h_x + h_y)}{h^5} \right] k dk, \\
&\approx -\frac{5\delta^3 e^3}{16\pi^2\hbar} \int_0^{2\pi} d\phi \int_{k_F-}^{k_F+} \left[\frac{8\delta^3 k^4 (\cos\phi - \sin\phi)^3}{|\Delta|^7} - \frac{12\Delta\delta^2 k^3 (\cos\phi - \sin\phi)^2 \sin\theta (\cos\varphi + \sin\varphi)}{|\Delta|^7} \right. \\
&\quad \left. - \frac{4\delta k^2 (\cos\phi - \sin\phi)}{|\Delta|^5} + \frac{2\Delta k \sin\theta (\cos\varphi + \sin\varphi)}{|\Delta|^5} \right] dk \\
&\approx -\frac{5\delta^3 e^3 \sin\theta (\cos\varphi + \sin\varphi)}{16\pi^2\hbar} \int_0^{2\pi} d\phi \int_{k_F-}^{k_F+} \left[\frac{2\Delta k}{|\Delta|^5} - \frac{12\Delta\delta^2 k^3 (\cos\phi - \sin\phi)^2}{|\Delta|^7} \right] dk \\
&\approx -\frac{5\delta^3 e^3 \Delta \sin\theta (\cos\varphi + \sin\varphi)}{8\pi^2\hbar |\Delta|^5} \left(-\frac{16\sqrt{2m_e^3\epsilon_F}|\delta|}{\hbar^3} - \frac{32\sqrt{2m_e^5}\delta^3}{3\hbar^5\sqrt{\epsilon_F}} + \frac{256\sqrt{2m_e^5\epsilon_F^3}|\delta|^3}{\hbar^5\Delta^2} + \frac{3072\sqrt{2m_e^7\epsilon_F}|\delta|^5}{3\hbar^7\Delta^2} + \frac{24576\sqrt{2m_e^9}|\delta|^7}{35\hbar^9\Delta^2\sqrt{\epsilon_F}} \right) \\
&= -\frac{\sigma_P^{\text{QM}}}{2\sqrt{2}} \sin\theta \sin(\varphi + \frac{\pi}{4}).
\end{aligned} \tag{A27}$$

In Eq. (A27), we have used the zero-order approximation for k_{Fs} , that is, $k_{Fs} \approx \sqrt{k_\phi^2 + k_0^2} - sk_\phi$ with $k_\phi = \sqrt{2m_e}|\delta(\cos\phi - \sin\phi)|/\hbar^2$ and $k_0 = \sqrt{2m_e\epsilon_F}/\hbar^2$. We substitute in Eq. (10) and find that

$$\begin{aligned}
\sigma_{\phi\phi}^{\text{QM}} &= \sigma_{xxx}^{\text{QM}} \cos^3\phi - \sigma_{xxx}^{\text{QM}} \sin^3\phi + 3\sigma_{xxx}^{\text{QM}} \sin^2\phi \cos\phi - 3\sigma_{xxx}^{\text{QM}} \sin\phi \cos^2\phi \\
&= \sigma_{xxx}^{\text{QM}} (\cos\phi - \sin\phi)^3 = -2\sqrt{2}\sigma_{xxx}^{\text{QM}} \sin^3(\phi - \frac{\pi}{4}) \\
&\approx \sigma_P^{\text{QM}} \sin\theta \sin(\varphi + \frac{\pi}{4}) \sin^3(\phi - \frac{\pi}{4}).
\end{aligned} \tag{A28}$$

- [1] A. Shapere and F. Wilczek, *Geometric Phases in Physics* (World Scientific, Singapore, 1989)
- [2] D. Xiao, M.-C. Chang, and Q. Niu, Berry phase effects on electronic properties, *Rev. Mod. Phys.* **82**, 1959 (2010).
- [3] Z. Z. Du, H.-Z. Lu, and X. C. Xie, Nonlinear Hall effects, *Nat. Rev. Phys.* **3**, 744 (2021).
- [4] P. Törmä, Essay: Where Can Quantum Geometry Lead Us?, *Phys. Rev. Lett.* **131**, 240001 (2023).
- [5] T. Liu, X.-B. Qiang, H.-Z. Lu, and X. C. Xie, Quantum geometry in condensed matter, *Natl. Sci. Rev.* **12**, nwae334 (2024).
- [6] M. Suárez-Rodríguez, F. de Juan, I. Souza, M. Gobbi, F. Casanova, and L. E. Hueso, Nonlinear transport in non-centrosymmetric systems, *Nat. Mater.* (2025).
- [7] I. Sodemann and L. Fu, Quantum nonlinear Hall effect induced

- by Berry curvature dipole in time-reversal invariant materials, Phys. Rev. Lett. **115**, 216806 (2015).
- [8] Y. Zhang, Y. Sun, and B. Yan, Berry curvature dipole in Weyl semimetal materials: An ab initio study, Phys. Rev. B **97**, 041101(R) (2018).
- [9] Q. Ma, S.-Y. Xu, H. Shen, D. MacNeill, V. Fatemi, T.-R. Chang, A. M. Mier Valdivia, S. Wu, Z. Du, C.-H. Hsu, S. Fang, Q. D. Gibson, K. Watanabe, T. Taniguchi, R. J. Cava, E. Kaxiras, H.-Z. Lu, H. Lin, L. Fu, N. Gedik, and P. JarilloHerrero, Observation of the nonlinear Hall effect under time-reversal-symmetric conditions, Nature (London) **565**, 337 (2019).
- [10] K. Kang, T. Li, E. Sohn, J. Shan, and K. F. Mak, Nonlinear anomalous Hall effect in few-layer WTe₂, Nat. Mater. **18**, 324 (2019).
- [11] A. Tiwari, F. Chen, S. Zhong, E. Druke, J. Koo, A. Kaczmarek, C. Xiao, J. Gao, X. Luo, Q. Niu *et al.*, Giant *c*-axis nonlinear anomalous Hall effect in *T*_d-MoTe₂ and WTe₂, Nat. Commun. **12**, 2049 (2021).
- [12] Y. Gao, S. A. Yang, and Q. Niu, Field induced positional shift of Bloch electrons and its dynamical implications, Phys. Rev. Lett. **112**, 166601 (2014).
- [13] C. Wang, Y. Gao, and D. Xiao, Intrinsic nonlinear Hall effect in antiferromagnetic tetragonal CuMnAs, Phys. Rev. Lett. **127**, 277201 (2021).
- [14] H. Liu, J. Zhao, Y.-X. Huang, W. Wu, X.-L. Sheng, C. Xiao, and S. A. Yang, Intrinsic second-order anomalous Hall effect and its application in compensated antiferromagnets, Phys. Rev. Lett. **127**, 277202 (2021).
- [15] A. Gao, Y.-F. Liu, J.-X. Qiu, B. Ghosh, T. V. Trevisan, Y. Onishi, C. Hu, T. Qian, H.-J. Tien, S.-W. Chen *et al.*, Quantum metric nonlinear Hall effect in a topological antiferromagnetic heterostructure, Science **381**, 181 (2023).
- [16] J. Wang, H. Zeng, W. Duan, and H. Huang, Intrinsic Nonlinear Hall Detection of the Néel Vector for Two-Dimensional Antiferromagnetic Spintronics, Phys. Rev. Lett. **131**, 056401 (2023).
- [17] Y. Fang, J. Cano, and S. Ali Akbar Ghorashi, Quantum Geometry Induced Nonlinear Transport in Altermagnets, Phys. Rev. Lett. **133**, 106701 (2024).
- [18] L. Xiang, B. Wang, Y. Wei, Z. Qiao, and J. Wang, Linear displacement current solely driven by the quantum metric, Phys. Rev. B **109**, 115121 (2024).
- [19] K. Das, S. Lahiri, R. B. Atencia, D. Culcer, and A. Agarwal, Intrinsic nonlinear conductivities induced by the quantum metric, Phys. Rev. B **108**, L201405 (2023).
- [20] D. Kaplan, T. Holder, and B. Yan, Unification of Nonlinear Anomalous Hall Effect and Nonreciprocal Magnetoresistance in Metals by the Quantum Geometry, Phys. Rev. Lett. **132**, 026301 (2024).
- [21] M. Ezawa, Intrinsic nonlinear conductivity induced by quantum geometry in altermagnets and measurement of the in-plane Néel vector, Phys. Rev. B **110**, L241405 (2024).
- [22] N. Wang, D. Kaplan, Z. Zhang, T. Holder, N. Cao, A. Wang, X. Zhou, F. Zhou, Z. Jiang, C. Zhang, S. Ru, H. Cai, K. Watanabe, T. Taniguchi, B. Yan, and W. Gao, Quantum-metric-induced nonlinear transport in a topological antiferromagnet, Nature (London) **621**, 487 (2023).
- [23] R. Wakatsuki, Y. Saito, S. Hoshino, Y. M. Itahashi, T. Ideue, M. Ezawa, Y. Iwasa, and N. Nagaosa, Nonreciprocal charge transport in noncentrosymmetric superconductors, Sci. Adv. **3**, e1602390 (2017).
- [24] Y. Tokura and N. Nagaosa, Nonreciprocal responses from noncentrosymmetric quantum materials, Nat. Commun. **9**, 3740 (2018).
- [25] M. Nadeem, M. S. Fuhrer, and X. Wang, The superconducting diode effect, Nat. Rev. Phys. **5**, 558 (2023).
- [26] J. Železný, Z. Fang, K. Olejník, J. Patchett, F. Gerhard, C. Gould, L. W. Molenkamp, C. Gomez-Olivella, J. Zemen, T. Tichý, T. Jungwirth, and C. Ciccarelli, Unidirectional magnetoresistance and spin-orbit torque in NiMnSb, Phys. Rev. B **104**, 054429 (2021).
- [27] W. Chen, M. Gu, J. Li, P. Wang, and Q. Liu, Role of Hidden Spin Polarization in Nonreciprocal Transport of Antiferromagnets, Phys. Rev. Lett. **129**, 276601 (2022).
- [28] H. J. Zhao, L. Tao, Y. Fu, L. Bellaiche, and Y. Ma, General Theory for Longitudinal Nonreciprocal Charge Transport, Phys. Rev. Lett. **133**, 096802 (2024).
- [29] T. Ideue, K. Hamamoto, S. Koshikawa, M. Ezawa, S. Shimizu, Y. Kaneko, Y. Tokura, N. Nagaosa, and Y. Iwasa, Bulk rectification effect in a polar semiconductor, Nat. Phys. **13**, 578 (2017).
- [30] Y. Li, Y. Li, P. Li, B. Fang, X. Yang, Y. Wen, D.-x. Zheng, C.-h. Zhang, X. He, A. Manchon, Z.-H. Cheng, and X.-x. Zhang, Nonreciprocal charge transport up to room temperature in bulk Rashba semiconductor α -GeTe, Nat. Commun. **12**, 540 (2021).
- [31] M. Kocsis, O. Zheliuk, P. Makk, E. Tóvári, P. Kun, O. E. Tereshchenko, K. A. Kokh, T. Taniguchi, K. Watanabe, J. Ye, and S. Csonka, In situ tuning of symmetry-breaking-induced nonreciprocity in the giant-Rashba semiconductor BiTeBr, Phys. Rev. Res. **3**, 033253 (2021).
- [32] R. Yoshimi, M. Kawamura, K. Yasuda, A. Tsukazaki, K. S. Takahashi, M. Kawasaki, and Y. Tokura, Nonreciprocal electrical transport in the multiferroic semiconductor (Ge,Mn)Te, Phys. Rev. B **106**, 115202 (2022).
- [33] Y. Wang, H. F. Legg, T. Bömerich, J. Park, S. Biesenkamp, A. A. Taskin, M. Braden, A. Rosch, and Y. Ando, Gigantic Magnetochiral Anisotropy in the Topological Semimetal Zr₂Te₅, Phys. Rev. Lett. **128**, 176602 (2022).
- [34] M. Suárez-Rodríguez, B. Martín-García, W. Skowroński, F. Calavalle, S. S. Tsirkin, I. Souza, F. De Juan, A. Chuvilin, A. Fert, M. Gobbi, F. Casanova, and L. E. Hueso, Odd Nonlinear Conductivity under Spatial Inversion in Chiral Tellurium, Phys. Rev. Lett. **132**, 046303 (2024).
- [35] M. Kondo, M. Kimata, M. Ochi, T. Kaneko, K. Kuroki, K. Sudo, S. Sakaguchi, H. Murakawa, N. Hanasaki, and H. Sakai, Nonreciprocal charge transport in polar Dirac metals with tunable spin-valley coupling, Phys. Rev. Research **7**, 013041 (2025).
- [36] X. Chen, Y. Fu, X. Wang, Y. Sui, H. J. Zhao, and L. L. Tao, Magnetic control of nonreciprocal charge transport, Phys. Rev. B **111**, 155411 (2025).
- [37] L. Tao and E. Y. Tsymbal, Insulator-to-conductor transition driven by the Rashba-Zeeman effect, npj Comput. Mater. **6**, 172 (2020).
- [38] I. Žutić, A. Matos-Abiague, B. Scharf, H. Dery, and K. Belashchenko, Proximity-induced materials, Mater. Today **22**, 85 (2019).
- [39] L. L. Tao and E. Y. Tsymbal, Spin-orbit dependence of anisotropic current-induced spin polarization, Phys. Rev. B **104**, 085438 (2021).
- [40] E. I. Rashba, Properties of semiconductors with an extremum loop .1. Cyclotron and combinational resonance in a magnetic field perpendicular to the plane of the loop, Sov. Phys. Solid State **2**, 1109 (1960).
- [41] D. Di Sante, P. Barone, R. Bertacco, and S. Picozzi, Electric Control of the Giant Rashba Effect in Bulk GeTe, Adv. Mater. **25**, 509 (2013).
- [42] A. Narayan, Class of Rashba ferroelectrics in hexagonal semiconductors, Phys. Rev. B **92**, 220101(R) (2015).

- [43] G. Dresselhaus, Spin-Orbit Coupling Effects in Zinc Blende Structures, *Phys. Rev.* **100**, 580 (1955).
- [44] L. G. D. da Silveira, P. Barone, and S. Picozzi, Rashba-Dresselhaus spin-splitting in the bulk ferroelectric oxide BiAlO_3 , *Phys. Rev. B* **93**, 245159 (2016).
- [45] L. L. Tao, T. R. Paudel, A. A. Kovalev, and E. Y. Tsymbal, Reversible spin texture in ferroelectric HfO_2 , *Phys. Rev. B* **95**, 245141 (2017).
- [46] M. Sakano, M. Hirayama, T. Takahashi, S. Akebi, M. Nakayama, K. Kuroda, K. Taguchi, T. Yoshikawa, K. Miyamoto, T. Okuda *et al.*, Radial Spin Texture in Elemental Tellurium with Chiral Crystal Structure, *Phys. Rev. Lett.* **124**, 136404 (2020).
- [47] G. Gatti, D. Gosálbez-Martínez, S. S. Tsirkin, M. Fanciulli, M. Puppin, S. Polishchuk, S. Moser, L. Testa, E. Martino, S. Roth *et al.*, Radial Spin Texture of the Weyl Fermions in Chiral Tellurium, *Phys. Rev. Lett.* **125**, 216402 (2020).
- [48] W. Tan, X. Jiang, Y. Li, X. Wu, J. Wang, and B. Huang, A Unified Understanding of Diverse Spin Textures of Kramers-Weyl Fermions in Nonmagnetic Chiral Crystals, *Adv. Funct. Mater.* **32**, 2208023 (2022).
- [49] B. A. Bernevig, J. Orenstein, and S. C. Zhang, Exact SU(2) Symmetry and Persistent Spin Helix in a Spin-Orbit Coupled System, *Phys. Rev. Lett.* **97**, 236601 (2006).
- [50] J. Schliemann, *Colloquium*: Persistent spin textures in semiconductor nanostructures, *Rev. Mod. Phys.* **89**, 011001 (2017).
- [51] M. Kohda and G. Salis, Physics and application of persistent spin helix state in semiconductor heterostructures, *Semicond. Sci. Technol.* **32**, 073002 (2017).
- [52] L. L. Tao and E. Y. Tsymbal, Persistent spin texture enforced by symmetry, *Nat. Commun.* **9**, 2763 (2018).
- [53] H. Lee, J. Im, and H. Jin, Emergence of the giant out-of-plane Rashba effect and tunable nanoscale persistent spin helix in ferroelectric SnTe thin films, *Appl. Phys. Lett.* **116**, 022411 (2020).
- [54] J. Sławińska, F. T. Cerasoli, P. Gopal, M. Costa, S. Curtarolo, and M. B. Nardelli, Ultrathin SnTe films as a route towards all-in-one spintronics devices, *2D Mater.* **7**, 025026 (2020).
- [55] L. L. Tao, M. Dou, X. Wang, and E. Y. Tsymbal, Ferroelectric spin-orbit valve effect, *Phys. Rev. Lett.* **134**, 076801 (2025).
- [56] L. L. Tao and E. Y. Tsymbal, Perspectives of spin-textured ferroelectrics, *J. Phys. D* **54**, 113001 (2021).
- [57] M. Dou, H. Li, and L. L. Tao, Spin relaxation in persistent spin textures, *New J. Phys.* **26**, 123005 (2024).
- [58] J. Callaway, *Quantum Theory of the Solid State* (Academic Press, San Diego, CA, 1991).
- [59] H. Watanabe and Y. Yanase, Nonlinear electric transport in odd-parity magnetic multipole systems: Application to Mn-based compounds, *Phys. Rev. Res.* **2**, 043081 (2020).
- [60] Y. Michishita and N. Nagaosa, Dissipation and geometry in nonlinear quantum transports of multiband electronic systems, *Phys. Rev. B* **106**, 125114 (2022).
- [61] Y. Wang, Z. Zhang, Z.-G. Zhu, and G. Su, Intrinsic nonlinear Ohmic current, *Phys. Rev. B* **109**, 085419 (2024).